Iranian Journal of Numerical Analysis and Optimization
Vol. 13, No. 2, 2023, pp 336–353
https://doi.org/10.22067/ijnao.2022.73126.1069
https://ijnao.um.ac.ir/

Research Article

An operational matrix method for solving a class of nonlinear Volterra integral equations arising in steady activation of a skeletal muscle

S. Torkaman*, M. Heydari and G.B. Loghmani

Abstract

The problem of the steady activation of a skeletal muscle is one of the applicable phenomena in real life that can be modeled by a Volterra integral equation. The current research aims to investigate this problem by using an effective operational matrix-based method. For this purpose, the operational matrix of integration is derived for the barycentric rational cardinal basis functions. Then, by utilizing the obtained operational matrix and without using any collocation points, the governing integral equation is reduced to a system of nonlinear algebraic equations. Convergence analysis of the proposed numerical method is studied thoroughly. Moreover, the obtained numerical results based on the proposed method with acceptable computational times support the theoretical results and reveal the accuracy and efficiency of the method.

AMS subject classifications (2020): Primary 45D05, Secondary 42C10, 65G99.

Keywords: Volterra integral equations; Linear barycentric rational interpolants; Operational matrix.

---

*Corresponding author

Received 17 October 2021; revised 17 August 2022; accepted 15 December 2022

Sorayya Torkaman
Department of Mathematical Sciences, Yazd University, Yazd, Iran.
e-mail: s.torkaman2009@gmail.com

Mohammad Heydari
Department of Mathematical Sciences, Yazd University, Yazd, Iran.
e-mail: m.heydari@yazd.ac.ir

Ghasem Barid Loghmani
Department of Mathematical Sciences, Yazd University, Yazd, Iran.
e-mail: loghmani@yazd.ac.ir

1 Introduction

Mathematical modeling of most problems in mechanics, mathematical biology, and economics are expressed as integral equations. Skeletal or striated muscles are one of the three types of muscles in the body. They connect to bones and control body movements, maintain body posture, protect internal organs, support the entry and exit points of the body, and regulate body temperature. The steady activation of a skeletal muscle is a phenomenon with complex and subtle physiological processes that can be described by Volterra integral equations (VIEs) [5, 8, 10]. The motor units (MUs) develop a skeletal muscle; each MUs contains a motoneuron (MN) and the muscle fibers it innervates. Electrical signals, coming from higher motor centers and propagating to the motoneurons along with a network of nerve fibers, compose the input of MUs. In this problem, MUs are ordered according to their maximal (tetanic) contraction forces t. Consider the muscle force $f(t)$ as a function of the last recruited MU for an arbitrary but fixed network. Clearly, $f(t)$ is an increasing function of t. As mentioned in [5, 8], the muscle force $f(t)$ can be stated with the following VIE:

$$f(t) = \int_a^t k(s, f(s), f(t))ds. \tag{1}$$

Equation (1) is a subclass of VIEs and can be called non-standard VIEs because, in addition to $f(s)$, its kernel also includes $f(t)$. Let ρ be a density function that represents the MU population. Suppose that $t_{\min}$ and $t_{\max}$ be the tetanic forces of the weakest and strongest MUs and let $\int_{t_{\min}}^{t_{\max}} \rho(s)ds$ be the number of MUs in the pool. The VIE for (1) takes the form [5]

$$f(v) = \int_{t_{\min}}^{v} K(f(v), f(u))h(u)du, \quad v \in [t_{\min}, t_{\max}], \tag{2}$$

where

$$K(f(v), f(u)) = 1 - c\exp\Big(- \alpha\frac{f(v) - f(u)}{f(u) + \Delta}\Big),$$

and $h(v) = v\rho(v)$, $\alpha > 0$, $\Delta > 0$, and $0 < c < 1$. The integral equation (2) governs the activation of a muscle, and it is not clear whether this equation has a solution or not. Because ρ is a strictly positive function almost everywhere, the function $H(t) = \int_{t_{\min}}^{t} h(s)ds$ is strictly increasing on the interval $[t_{\min}, t_{\max}]$ and hence invertible. $H(t)$ represents the force of the muscle when all MUs up to level t produce their tetanic force and $H(t_{\max}) = F_{\max}$. Now, by considering the change of variable $u = H^{-1}(x)$, the VIE (2) can be reduced to

$$f(v) = \int_{H(t_{\min})}^{H(v)} K(f(v), f(H^{-1}(x)))dx, \quad v \in [t_{\min}, t_{\max}]. \tag{3}$$

Then by assuming $H(v) = t$ and equivalently $v = H^{-1}(t)$, the integral equation (3) can be written as

$$Y(t) = \int_0^t \Big(1 - c\exp\Big(-\alpha\frac{Y(t)-Y(x)}{Y(x)+\Delta}\Big)\Big)dx, \quad t \in [0,T], \tag{4}$$

where $Y(t) = f(H^{-1}(t))$ and $T = F_{\max}$. Finally, the muscle force function can be obtained as $f(t) = Y(H(t))$. The existence and uniqueness of a non-negative solution of the VIE (4) are studied in [5].

The main purpose of this paper is to develop a computational method based on the linear barycentric rational interpolants (LBRIs) and associated integral operational matrix to approximate the problem of steady activation of a skeletal muscle (1). The LBRIs were introduced by Berrut [2] and then generalized by Floater and Hormann [4]. The family of Floater–Hormann (FH) interpolants has no real poles and has a high order of convergence for enough smooth functions. Furthermore, the FH interpolants offer a better choice than the polynomial interpolants, which are ill-conditioned and yield Runge's phenomenon in the case of equispaced interpolation nodes. Also, the LBRIs can be applied to approximate derivatives and integrals of a given function [1, 6]. Due to the attractive features of the LBRIs, many researchers are interested in developing numerical methods based on such interpolants to solve functional equations such as differential equations [13, 11], Volterra and Fredholm integral equations [3, 7], and integro-differential integral equations [1].

The paper is organized as follows: In Sections 2 and 3, the LBRIs and the corresponding integral operational matrix are described, respectively. In Section 4, the numerical technique for solving the VIE (1) based on the integral operational matrix is introduced. In Section 5, the convergence analysis of the proposed method is provided. In Section 6, the obtained numerical results are reported. Finally, a brief conclusion is given in Section 7.

2 The LBRIs

Let $n \in \mathbb{N}$, let $f : [a,b] \to \mathbb{R}$, let $\Omega = \{a \le t_0 < t_1 < \cdots < t_n \le b\}$ be a set of nodes on the interval $[a,b]$, and let $f(t_j),\ j = 0,1,\dots,n$ be the corresponding given data. The LBRIs can be defined as follows:

$$I_n(t) = \sum_{j=0}^{n} f(t_j)\phi_j(t), \tag{5}$$

where

$$\phi_j(t) = \frac{\frac{w_j}{t-t_j}}{\sum_{i=0}^{n}\frac{w_i}{t-t_i}}, \quad j = 0,1,\dots,n, \tag{6}$$

are barycentric cardinal basis functions with the following features:

- $\sum_{j=0}^{n} \phi_j(t) = 1,$
- $\phi_j(t_i) = \delta_{ij}, \quad i, j = 0, 1, \ldots, n,$

where δ_{ij} is the Kronecker delta. Also, the nonzero real numbers $\{w_j\}_{j=0}^{n}$ are barycentric weights independent of $f(t_j)$. Floater and Hormann [4] proposed a family of LBRIs by introducing w_j as

$$w_j = (-1)^j \sum_{i=\max(j-d,0)}^{\min(j,n-d)} \Big(\prod_{k=i,k\neq j}^{i+d} \frac{1}{\mid t_j - t_k \mid} \Big), \quad j = 0, 1, \ldots, n, \tag{7}$$

where $0 \le d \le n$ is an integer parameter. Using the barycentric weights (7), the LBRI (5) can be rewritten as follows [4]:

$$I_n(t) = \frac{\sum_{j=0}^{n-d} \lambda_j(t) p_j(t)}{\sum_{j=0}^{n-d} \lambda_j(t)}, \quad \lambda_j(t) = \frac{(-1)^j}{(t - t_j) \ldots (t - t_{j+d})}, \quad j = 0, 1, \ldots, n-d, \tag{8}$$

where $p_j(t)$ is the polynomial of degree at most d interpolates $f(t)$ at local nodes $\{x_{j+k}\}_{k=0}^{d}$. In [4], it is proved that the interpolant (8) has no real poles.

Theorem 1. [4] *Let $f \in C^{d+2}[a, b]$. Then*

$$\|f(t) - I_n(t)\|_\infty \le Ch^{d+1},$$

where

$$C = (1 + \gamma\mu) \begin{cases} (b-a)\frac{\|f^{(d+2)}\|_\infty}{d+2}, & (n-d) \text{ odd}, \\ \left((b-a)\frac{\|f^{(d+2)}\|_\infty}{d+2} + \frac{\|f^{(d+1)}\|_\infty}{d+1} \right), & (n-d) \text{ even}, \end{cases}$$

$$\mu = \max_{1\le i\le n-2} \min\left(\frac{t_{i+1} - t_i}{t_i - t_{i-1}}, \frac{t_{i+1} - t_i}{t_{i+2} - t_{i+1}} \right),$$

$$\gamma = \begin{cases} 1, \, d = 0, \\ 0, \, d > 1, \end{cases}, \qquad h = \max_{0\le i\le n-1} (t_{i+1} - t_i).$$

Similar to the one-dimensional LBRIs (6), one can define two-dimensional LBRIs. For this purpose, two-dimensional barycentric rational basis functions can be defined as

$$\psi_{ij}(t,s)=\phi_i(t)\phi_j(s),\quad i,j=0,1,\dots,n,$$

where $\{\phi_i(t)\}_{i=0}^n$ are the basis functions (6). The basis functions $\{\psi_{ij}(t,s)\}$ have the following properties:

- $\displaystyle\sum_{i=0}^{n}\sum_{j=0}^{n}\psi_{ij}(t,s)=1,$
- $\psi_{ij}(t_k,s_l)=\delta_{ik}\delta_{jl}.$

According to the Lagrange property, any two-dimensional function $f(t,s)$ can be approximated as

$$f(t,s)\simeq\sum_{i=0}^{n}\sum_{j=0}^{n}f(t_i,s_j)\psi_{ij}(t,s). \tag{9}$$

Also, by using the barycentric weights defined in (7), the two-dimensional LBRI (9) can be rewritten in the form of the two-dimensional FH interpolants as

$$I_n(t,s)=\frac{\displaystyle\sum_{i=0}^{n-d}\sum_{j=0}^{n-d}\lambda_i(t)\lambda_j(s)p_{i,j}(t,s)}{\displaystyle\sum_{i=0}^{n-d}\sum_{j=0}^{n-d}\lambda_i(t)\lambda_j(s)}, \tag{10}$$

where

$$\lambda_i(t)=\frac{(-1)^i}{(t-t_i)\dots(t-t_{i+d})},$$
$$\lambda_j(s)=\frac{(-1)^j}{(s-s_j)\dots(s-s_{j+d})},\quad i,j=0,1,\dots,n,$$

in which $p_{i,j}(t,s)$ is the polynomial that interpolates f at local nodes $\{(t_{i+k},s_{j+l})\}_{k,l=0}^d$. In the following, by applying Theorem 1, the error bound of the two-dimensional Floater–Hormann interpolant (10) is estimated.

Theorem 2. *Let $f(t,s)\in C^{d+2}([a,b]\times[a,b])$. Then*

$$\|f(t,s)-I_n(t,s)\|_\infty=O(h^{d+1}).$$

Proof. Suppose that

$$\Omega_t=\{a\le t_0<t_1<\cdots<t_n\le b\},$$
$$\Omega_s=\{a\le s_0<s_1<\cdots<s_n\le b\},$$

and let $\{(t_i,s_j)\}_{i,j=0}^{n}$ be the interpolation nodes on $[a,b]\times[a,b]$. Then

$$f(t,s)=I_n(t,s),\qquad \text{for all } (t,s)\in\Omega_t\times\Omega_s.$$

Now, the error interpolation can be written as

$$f(t,s)-I_n(t,s)=\frac{\displaystyle\sum_{i=0}^{n-d}\sum_{j=0}^{n-d}\lambda_i(t)\lambda_j(s)(f(t,s)-p_{ij}(t,s))}{\displaystyle\sum_{i=0}^{n-d}\sum_{j=0}^{n-d}\lambda_i(t)\lambda_j(s)},\tag{11}$$

for any $(t,s)\in[a,b]\times[a,b]-\Omega_t\times\Omega_s$. By extending the Newton form of polynomial interpolant error and using the commuting property of the divided differences described in [9], the Newton error formula for a two-dimensional polynomial interpolation can be represented as

$$\begin{aligned}f(t,s)-p_{ij}(t,s)=&\pi_{d+1}(t)[t_i,t_{i+1},\ldots,t_{i+d},t]f\\&+\pi_{d+1}(s)[s_j,s_{j+1},\ldots,s_{j+d},s]f\\&-\pi_{d+1}(t)\pi_{d+1}(s)[s_j,s_{j+1},\ldots,s_{j+d},s][t_i,t_{i+1},\ldots,t_{i+d},t]f,\end{aligned}\tag{12}$$

where $\pi_{d+1}(t)=\prod_{r=0}^{d}(t-t_{i+r})$ and $\pi_{d+1}(s)=\prod_{r=0}^{d}(s-s_{j+r})$. Replacing (12) in (11) yields

$$\begin{aligned}f(t,s)-I_n(t,s)=&\frac{\displaystyle\sum_{i=0}^{n-d}(-1)^i[t_i,t_{i+1},\ldots,t_{i+d},t]f}{\sum_{i=0}^{n-d}\lambda_i(t)}\\&+\frac{\displaystyle\sum_{j=0}^{n-d}(-1)^j[s_j,s_{j+1},\ldots,s_{j+d},s]f}{\sum_{j=0}^{n-d}\lambda_j(s)}\\&-\frac{\displaystyle\sum_{i=0}^{n-d}\sum_{j=0}^{n-d}(-1)^{i+j}[t_i,t_{i+1},\ldots,t_{i+d},t][s_j,s_{j+1},\ldots,s_{j+d},s]f}{\displaystyle\sum_{i=0}^{n-d}\sum_{j=0}^{n-d}\lambda_i(t)\lambda_j(s)}.\end{aligned}\tag{13}$$

To complete the proof, it is enough to compute an upper bound for the numerators and a lower bound for the denominators of the used quotient in (13). In [4], the upper bounds for the numerator of the first and second quotients applied in (13) are derived. Moreover, the following inequalities hold [4]:

$$\Big|\sum_{i=0}^{n-d}\lambda_i(t)\Big| \geq \frac{1}{(1+\gamma\mu)d!h^{d+1}}, \quad \Big|\sum_{j=0}^{n-d}\lambda_j(s)\Big| \geq \frac{1}{(1+\gamma\mu)d!h^{d+1}}, \tag{14}$$

where γ and μ are defined in Theorem 1. Now, it is enough to get an upper bound on the numerator of the third quotient in (13). Let $n-d$ be odd. Following the proof of Theorem 2 in [4], one can get

$$\begin{aligned}
&\sum_{i=0}^{n-d}\sum_{j=0}^{n-d}(-1)^{i+j}[t_i,t_{i+1},\ldots,t_{i+d},t][s_j,s_{j+1},\ldots,s_{j+d},s]f\\
&=-\sum_{i=0}^{n-d}\sum_{\substack{j=0\\ j \text{ even}}}^{n-d-1}(-1)^i(s_{j+d+1}-s_j)[t_i,t_{i+1},\ldots,t_{i+d},t][s_j,s_{j+1},\ldots,s_{j+d+1},s]f\\
&=\sum_{\substack{i=0\\ i \text{ even}}}^{n-d-1}\sum_{\substack{j=0\\ j \text{ even}}}^{n-d-1}(t_{i+d+1}-t_i)(s_{j+d+1}-s_j)\\
&\quad\times[t_i,t_{i+1},\ldots,t_{i+d+1},t][s_j,s_{j+1},\ldots,s_{j+d+1},s]f,
\end{aligned}$$

and therefore

$$\begin{aligned}
&\Big|\sum_{i=0}^{n-d}\sum_{j=0}^{n-d}(-1)^{i+j}[t_i,t_{i+1},\ldots,t_{i+d},t][s_j,s_{j+1},\ldots,s_{j+d},s]f\Big|\\
&\quad\leq\sum_{\substack{i=0\\ i \text{ even}}}^{n-d-1}\sum_{\substack{j=0\\ j \text{ even}}}^{n-d-1}\frac{|t_{i+d+1}-t_i||s_{j+d+1}-s_j|}{((d+2)!)^2}\Big|\frac{\partial^{2d+4}}{\partial t^{d+2}\partial s^{d+2}}f\Big|\\
&\quad\leq\frac{(d+1)^2(b-a)^2}{((d+2)!)^2}\Big\|\frac{\partial^{2d+4}}{\partial t^{d+2}\partial s^{d+2}}f\Big\|_\infty.
\end{aligned}\tag{15}$$

Let $n-d$ be even. In a similar manner, by following the proof of Theorem 2 in [4], the following result is obtained:

$$\begin{aligned}
&\sum_{i=0}^{n-d}\sum_{j=0}^{n-d}(-1)^{i+j}[t_i,t_{i+1},\ldots,t_{i+d},t][s_j,s_{j+1},\ldots,s_{j+d},s]f\\
&=\sum_{\substack{i=0\\ i \text{ even}}}^{n-d-2}\sum_{\substack{j=0\\ j \text{ even}}}^{n-d-2}(t_{i+d+1}-t_i)(s_{j+d+1}-s_j)\\
&\quad\times[t_i,t_{i+1},\ldots,t_{i+d+1},t][s_j,s_{j+1},\ldots,s_{j+d+1},s]f\\
&\quad-\sum_{\substack{i=0\\ i \text{ even}}}^{n-d-2}(t_{i+d+1}-t_i)[t_i,t_{i+1},\ldots,t_{i+d+1},t][s_{n-d},s_{n-d+1},\ldots,s_n,s]f
\end{aligned}$$

$$
\begin{aligned}
&- \sum_{\substack{j=0 \\ j \text{ even}}}^{n-d-2} (s_{j+d+1} - s_j)[t_{n-d}, t_{n-d+1}, \ldots, t_n, t][s_j, s_{j+1}, \ldots, s_{j+d+1}, s]f \\
&+ [t_{n-d}, t_{n-d+1}, \ldots, t_n, t][s_{n-d}, s_{n-d+1}, \ldots, s_n, s]f,
\end{aligned}
$$

and therefore

$$
\begin{aligned}
&\Big| \sum_{i=0}^{n-d} \sum_{j=0}^{n-d} (-1)^{i+j} [t_i, t_{i+1}, \ldots, t_{i+d}, t][s_j, s_{j+1}, \ldots, s_{j+d}, s]f \Big| \\
&\le \frac{(d+1)^2(b-a)^2}{((d+2)!)^2} \Big\| \frac{\partial^{2d+4}}{\partial t^{d+2} \partial s^{d+2}} f \Big\|_\infty + \frac{b-a}{d!(d+2)!} \Big\| \frac{\partial^{2d+3}}{\partial t^{d+2} \partial s^{d+1}} f \Big\|_\infty \\
&\quad + \frac{b-a}{d!(d+2)!} \Big\| \frac{\partial^{2d+3}}{\partial t^{d+1} \partial s^{d+2}} f \Big\|_\infty + \frac{1}{((d+1)!)^2} \Big\| \frac{\partial^{2d+2}}{\partial t^{d+1} \partial s^{d+1}} f \Big\|_\infty . \qquad (16)
\end{aligned}
$$

Finally, by using the relations (14), (15), and (16), the desired result can be obtained as follows:

• If $n-d$ is odd, then

$$
\begin{aligned}
\Big\| f(s,t) - I_n(s,t) \Big\|_\infty \le & \frac{(1+\gamma\mu)(b-a)}{d+2} \left(\Big\| \frac{\partial^{d+2}}{\partial t^{d+2}} f \Big\|_\infty + \Big\| \frac{\partial^{d+2}}{\partial s^{d+2}} f \Big\|_\infty \right) h^{d+1} \\
& + \frac{(1+\gamma\mu)^2(b-a)^2}{(d+2)^2} \Big\| \frac{\partial^{2d+4}}{\partial t^{d+2} \partial s^{d+2}} f \Big\|_\infty h^{2d+2}.
\end{aligned}
$$

• If $n-d$ is even, then

$$
\begin{aligned}
\Big\| f(t,s) - I_n(t,s) \Big\|_\infty \le & \frac{(1+\gamma\mu)(b-a)}{d+2} \left(\Big\| \frac{\partial^{d+2}}{\partial t^{d+2}} f \Big\|_\infty + \Big\| \frac{\partial^{d+2}}{\partial s^{d+2}} f \Big\|_\infty \right) h^{d+1} \\
& + \frac{1+\gamma\mu}{d+1} \left(\Big\| \frac{\partial^{d+1}}{\partial t^{d+1}} f \Big\|_\infty + \Big\| \frac{\partial^{d+1}}{\partial s^{d+1}} f \Big\|_\infty \right) h^{d+1} \\
& + \frac{(1+\gamma\mu)^2(b-a)^2}{(d+2)^2} \Big\| \frac{\partial^{2d+4}}{\partial t^{d+2} \partial s^{d+2}} f \Big\|_\infty h^{2d+2} \\
& + \frac{(1+\gamma\mu)^2}{(d+1)^2} \Big\| \frac{\partial^{2d+2}}{\partial t^{d+1} \partial s^{d+1}} f \Big\|_\infty h^{2d+2} \\
& + \frac{(1+\gamma\mu)^2(b-a)}{(d+1)(d+2)} h^{2d+2} \\
& \times \left(\Big\| \frac{\partial^{2d+3}}{\partial t^{d+2} \partial s^{d+1}} f \Big\|_\infty + \Big\| \frac{\partial^{2d+3}}{\partial t^{d+1} \partial s^{d+2}} f \Big\|_\infty \right).
\end{aligned}
$$

□

3 Integral operational matrix

In this section, a brief review of the integral operational matrix based on the barycentric rational basis functions described in [14, 12] is provided. Suppose that $\Phi(t)$ is an $(n+1)\times 1$ vector as follows:

$$\Phi(t) = [\phi_0(t), \phi_1(t), \ldots, \phi_n(t)]^T, \tag{17}$$

where $\phi_i(t),\ i = 0, 1, \ldots, n$, are defined in (6). The integration of vector $\Phi(t)$ in (17) can be expressed as

$$\int_a^t \Phi(s)ds = \Big[\int_a^t \phi_0(s)ds, \int_a^t \phi_1(s)ds, \ldots, \int_a^t \phi_n(s)ds\Big]^T. \tag{18}$$

Using (5), any elements of the vector (18) can be estimated as

$$\int_a^t \phi_i(s)ds \simeq \sum_{j=0}^{n} p_{ij}\phi_j(t) = \mathbf{P_i}\Phi(t), \quad i = 0, 1, \ldots, n. \tag{19}$$

where

$$\mathbf{P_i} = [p_{i0}, p_{i1}, \ldots, p_{in}], \quad i = 0, 1, \ldots, n.$$

Replacing (19) in (1) yields

$$\int_a^t \Phi(s)ds \simeq \Big[\mathbf{P_0}\Phi(t), \mathbf{P_1}\Phi(t), \ldots, \mathbf{P_n}\Phi(t)\Big]^T = \mathbf{P}\Phi(t),$$

in which

$$\mathbf{P} = \Big[\mathbf{P_0}, \mathbf{P_1}, \ldots, \mathbf{P_n}\Big]^T.$$

Hence, the operational matrix of integration can be defined as follows.

Definition 1. Let $\Phi(t)$ be the vector stated in (17). The operational matrix of integration $\mathbf{P}$, based on the barycentric basis functions, can be represented as

$$\int_a^t \Phi(s)ds \simeq \mathbf{P}\Phi(t),$$

where $\mathbf{P} = (p_{ij})$ and p_{ij} can be computed as

$$p_{ij} = \int_a^{t_j} \phi_i(s)ds, \quad i, j = 0, 1, \ldots, n.$$

Remark 1. Let A be an $(n+1)\times(n+1)$ matrix. Using (10), the function $\Phi^T(t)A\Phi(t)$ can be approximated as follows:

$$\Phi^T(t)A\Phi(t) \simeq \sum_{j=0}^{n} \Phi^T(t_j)A\Phi(t_j)\phi(t).$$

Due to the Lagrange property of the basis functions (6), one can get

$$\Phi^T(t)A\Phi(t) \simeq \hat{\mathbf{A}}\Phi(t), \quad \hat{\mathbf{A}} = [A_{00}, A_{11}, \dots, A_{nn}],$$

where $\hat{\mathbf{A}}$ is a row vector composed of the diagonal elements of matrix A.

4 Description of the numerical method

In this section, an operational matrix-based method will be discussed to solve the nonlinear VIE (1). For this purpose, by using (5), the function $f(t)$ is approximated as

$$f(t) \simeq f_n(t) = \sum_{i=0}^{n} f(t_i)\phi_i(t) = F^T\Phi(t), \tag{20}$$

where

$$F = [f(t_0), f(t_1), \dots, f(t_n)]^T,$$

is the unknown vector and should be determined to compute the approximate solution of the problem. At first, using (20), the function $k(s, f_n(s), f_n(t))$ is estimated respect to the variable s as

$$k\Big(s, f_n(s), f_n(t)\Big) \simeq K(t)^T\Phi(s), \tag{21}$$

where

$$K(t) = \Big[k\Big(s_0, f_n(s_0), f_n(t)\Big), k\Big(s_1, f_n(s_1), f_n(t)\Big), \dots, k\Big(s_n, f_n(s_n), f_n(t)\Big)\Big]^T,$$

and $s_i = t_i, \ i = 0, 1, \dots, n$. From (20) and according to the Lagrange property of the basis functions $\phi_i(t), \ i = 0, 1, \dots, n$, the vector $K(t)$ can be rewritten as

$$K(t) = \Big[k\Big(s_0, f(s_0), f_n(t)\Big), k\Big(s_1, f(s_1), f_n(t)\Big), \dots, k\Big(s_n, f(s_n), f_n(t)\Big)\Big]^T.$$

Again using (5), each component of the vector $K(t)$ is approximated as

$$k\Big(s_i, f(s_i), f_n(t)\Big) \simeq K_i^T \Phi(t), \quad i = 0, 1, \ldots, n, \tag{22}$$

where

$$K_i = \Big[k\Big(s_i, f(s_i), f(t_0)\Big), k\Big(s_i, f(s_i), f(t_1)\Big), \ldots, k\Big(s_i, f(s_i), f(t_n)\Big)\Big]^T.$$

Substituting (22) into (21) yields

$$k\Big(s, f_n(s), f_n(t)\Big) \simeq \Phi^T(t) K^T \Phi(s), \tag{23}$$

where K is a $(n+1) \times (n+1)$ matrix and $K_{ij} = k(s_i, f(s_i), f(t_j))$. Now, by substituting (20) and (23) into (1), one can obtain

$$F^T \Phi(t) - \Phi(t)^T K^T \int_a^t \Phi(s) ds = 0.$$

Using the integral operational matrix defined in Definition 1, we arrive at

$$F^T \Phi(t) - \Phi(t)^T K^T \mathbf{P} \Phi(t) = 0. \tag{24}$$

Finally, applying Remark 1 leads to the following nonlinear algebraic system:

$$F^T - \hat{\mathbf{A}} = 0, \tag{25}$$

where $\hat{\mathbf{A}}$ is a row vector constructed of the diagonal elements of the matrix $K^T\mathbf{P}$. Thus, the unknown vector F can be computed by solving the nonlinear system of algebraic equations (25).

5 Convergence analysis

In this section, the convergence analysis of the proposed numerical scheme is presented. To this end, we utilize the following norms to measure the approximation error:

$\|v(t)\|_\infty = \max_{t \in [a,b]} v(t)$, for real function $v : [a, b] \to \mathbb{R}$,

$\|V(t)\|_\infty = \max_{1 \le i \le k} \|v_i(t)\|_\infty$, for vector function $V(t) = [v_1(t), v_2(t), \ldots, v_k(t)]^T$,

$v_i : [a, b] \to \mathbb{R}$.

Lemma 1. *Let $\Phi(t)$ be the vector defined in (17) with the weights (7). Then,*

$$\Big\| \int_a^t \Phi(s) ds - \mathbf{P}\Phi(t) \Big\|_\infty = O(h^{d+1}).$$

Proof. By integrating from the vector $\Phi(t)$, one obtains

$$\Big\| \int_a^t \Phi(s)ds - \mathbf{P}\Phi(t) \Big\|_\infty = \max_{0\le i\le n} \Big| \int_a^t \phi_i(s)ds - \mathbf{P_i}\Phi(t) \Big|, \tag{26}$$

where $\mathbf{P_i}$ is the ith row of the integral operational matrix $\mathbf{P}$. According to (19) and Theorem 1, one can get

$$\Big\| \int_a^t \phi_i(s)ds - \mathbf{P_i}\Phi(t) \Big\|_\infty \le h^{d+1}(1+\gamma\mu) \\ \times \begin{cases} (b-a)\frac{\|\phi_i^{(d+2)}\|_\infty}{d+2}, & (n-d) \text{ odd} \\ \left((b-a)\frac{\|\phi_i^{(d+2)}\|_\infty}{d+2} + \frac{\|\phi_i^{(d+1)}\|_\infty}{d+1}\right), & (n-d) \text{ even} \end{cases} \tag{27}$$

Substituting (27) into (26), the desired result is obtained as

$$\Big\| \int_a^t \Phi(s)ds - \mathbf{P}\Phi(t) \Big\|_\infty \le Ch^{d+1},$$

where

$$C = (1+\gamma\mu) \begin{cases} (b-a)\frac{\|\Phi^{(d+2)}\|_\infty}{d+2}, & (n-d) \text{ odd} \\ \left((b-a)\frac{\|\Phi^{(d+2)}\|_\infty}{d+2} + \frac{\|\Phi^{(d+1)}\|_\infty}{d+1}\right), & (n-d) \text{ even} \end{cases}$$

and

$$\Phi^{(d)}(t) = [\phi_0^{(d)}(t), \phi_1^{(d)}(t), \dots, \phi_n^{(d)}(t)]^T, \qquad \| \Phi^{(d)}(t) \|_\infty = \max_{0\le i\le n} |\phi_i^{(d)}(t)|.$$

□

Lemma 2. *Consider A an $(n+1)\times(n+1)$ matrix, and let $\Phi(t)$ be the vector defined in (17) with the weights (7). Then,*

$$\|\Phi^T(t)A\Phi(t) - \hat{\mathbf{A}}\Phi(t)\|_\infty = O(h^{d+1}),$$

where $\hat{\mathbf{A}}$ is a row vector composed of the diagonal elements of the matrix A.

Proof. As mentioned in Remark 1, we have

$$\Phi^T(t)A\Phi(t) \simeq \hat{\mathbf{A}}\Phi(t).$$

Finally, by applying the weights (7) and using Theorem 1, the desired result is acquired. □

Theorem 3. *Let $f \in C^{d+2}[a,b]$, let $k \in C^{d+2}([a,b],\mathbb{R},\mathbb{R})$, and let the kernel k satisfy the following Lipschitz condition:*

$$|k(s,y_1,z_1) - k(s,y_2,z_2)| \leq L(|y_1-y_2| + |z_1-z_2|),$$
$$\text{for all } (s,y_1,z_1),(s,y_2,z_2) \in [a,b]\times\mathbb{R}^2.$$

Also, consider $f_n(t) = F^T\Phi(t)$ the approximate solution of (1) such that F is obtained from solving the nonlinear system of algebraic equations (25) and $2L(b-a) < 1$. Then

$$\|f(t) - f_n(t)\|_\infty \to 0, \quad \text{as} \quad n \to +\infty.$$

Proof. The residual function of the VIE (1) can be computed as follows:

$$\mathbf{RES}_n(t) = f_n(t) - \int_a^t k\Big(s, f_n(s), f_n(t)\Big)ds. \tag{28}$$

Now, by subtracting relation (24) from (28) and utilizing equation (25), the residual function $\mathbf{RES}_n(t)$ can be rewritten as

$$\mathbf{RES}_n(t) = \underbrace{(F^T - \hat{\mathbf{A}})}_{0}\Phi(t) - \int_a^t \Big(k\Big(s, f_n(s), f_n(t)\Big) - \Phi^T(t)K^T\Phi(s)\Big)ds$$
$$-\Phi^T(t)K^T\Big(\int_a^t \Phi(s)ds - \mathbf{P}\Phi(t)\Big) - (\Phi^T(t)K^T\mathbf{P}\Phi(t) - \hat{\mathbf{A}}\Phi(t)).$$

Therefore

$$\begin{aligned}\|\mathbf{RES}_n(t)\|_\infty \leq{}& (b-a)\Big\|k\Big(s, f_n(s), f_n(t)\Big) - \Phi^T(t)K^T\Phi(s)\Big\|_\infty\\ &+\|\Phi^T(t)K^T\|_\infty\Big\|\int_a^t \Phi(s)ds - \mathbf{P}\Phi(t)\Big\|_\infty\\ &+\|\Phi^T(t)K^T\mathbf{P}\Phi(t) - \hat{\mathbf{A}}\Phi(t)\|_\infty,\end{aligned}$$

Employing Theorem 2, and Lemmas 1 and 2 leads to the following relation:

$$\|\mathbf{RES}_n(t)\|_\infty = O(h^{d+1}). \tag{29}$$

Let $E_n(t) = f(t) - f_n(t)$. Substituting $f(t) = f_n(t) + E_n(t)$ into the VIE (1), one can obtain

$$f_n(t) + E_n(t) = \int_a^t k\Big(s, f_n(s) + E_n(s), f_n(t) + E_n(t)\Big)ds. \tag{30}$$

Employing the residual function (28) and relation (30) yields the following equation:

$$E_n(t) = \int_a^t \Big(k(s, f_n(s) + E_n(s), f_n(t) + E_n(t)) - k(s, f_n(s), f_n(t)) \Big) ds$$
$$-\mathbf{RES}_n(t).$$

Therefore

$$|E_n(t)| \leq \int_a^t \Big| k(s, f_n(s) + E_n(s), f_n(t) + E_n(t)) - k(s, f_n(s), f_n(t)) \Big| ds$$
$$+|\mathbf{RES}_n(t)|.$$

Finally, applying the Lipschitz condition yields

$$|E_n(t)| \leq L \int_a^t (|E_n(s)| + |E_n(t)|) ds + |\mathbf{RES}_n(t)|,$$

and consequently

$$\|E_n(t)\|_\infty \leq \frac{\|\mathbf{RES}_n(t)\|_\infty}{1 - 2L(b-a)}.$$

From (29) and $2L(b-a) < 1$, the desired result is obtained as

$$\|E_n(t)\|_\infty \to 0 \quad \text{as} \quad h \to 0.$$

□

6 Numerical results

In this section, the proposed method is applied based on the integral operational matrix to approximate the solution of the VIE (4). Consider $t_{\min} = 10$, $t_{\max} = 20$, $c = 0.9$, $\alpha = 1.14$, and $\rho(t) = \frac{1}{t}$, $t \in [t_{\min}, t_{\max}]$. To get the numerical results, the equidistant nodes are employed on the interval $[0, 10]$, and the algorithm associated with the proposed method is implemented using Maple 2015 software on a Core (TM) i7 PC with 2.70 GHz of CPU and 16 GB of RAM. Here, the fsolve command is used to solve the nonlinear system (25). Also, the rate of convergence of the numerical method is determined based on the following formula:

$$\text{Ratio} = \frac{\log(\|E_n\|_\infty) - \log(\|E_{n'}\|_\infty)}{\log(h) - \log(h')}, \tag{31}$$

where h and h' are defined in Theorem 1. Because the exact solution of (4) is unknown, we use the error of residual function to verify the efficiency and high accuracy of the proposed method. So, to commutating the rate of convergence of the method, the absolute error $E_n(t)$ in (31) is replaced by the error of residual function $\mathbf{RES}_n(t)$.

Figure 1 depicts the approximation solution $Y_n(t)$ and the residual function $|\mathbf{RES}_n(t)|$ with $n = 20$ and $d = 18$ for different values of Δ.

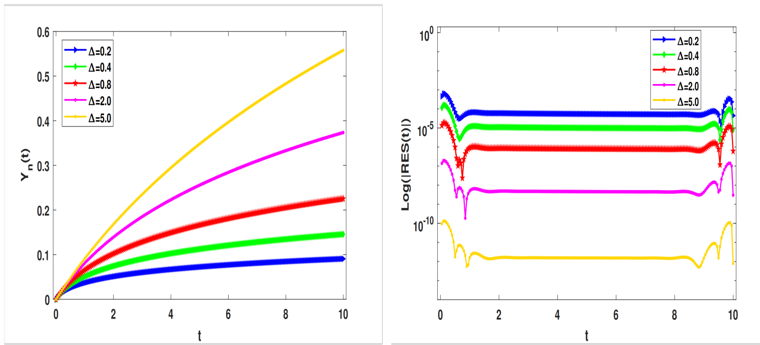

Figure 1: Graphs of $Y(t)$ and $|\mathbf{RES_n(t)}|$ with $n = 20$ and $d = 18$

Table 1 reports the numerical results for the VIE (4) for $\Delta = 2$, 5, and 10.

Table 1: Numerical results with $n = 20$ and $d = 19$

t	$\lvert\mathbf{RES}_n(t)\rvert$		
	$\Delta = 2$	$\Delta = 5$	$\Delta = 10$
0.0	0.000000	0.0000000	0.0000000
1.0	$3.98e-9$	$9.53e-13$	$1.67e-16$
2.0	$3.90e-9$	$9.46e-13$	$1.66e-16$
3.0	$3.82e-9$	$9.34e-13$	$1.65e-16$
4.0	$3.75e-9$	$9.23e-13$	$1.64e-16$
5.0	$3.69e-9$	$9.14e-13$	$1.63e-16$
6.0	$3.64e-9$	$9.05e-13$	$1.62e-16$
7.0	$3.60e-9$	$8.97e-13$	$1.63e-16$
8.0	$3.56e-9$	$8.80e-13$	$1.72e-16$
9.0	$3.51e-9$	$8.80e-13$	$2.21e-16$
10	$2.44e-9$	$4.74e-13$	$3.33e-16$
CPU time (s)	2.121	2.043	2.184

Table 2 represents the residual function error and the convergence rate for different values of d. According to this table, one can infer that the order of convergence is ≈ 4 for $d = 3$ and ≈ 3 for $d = 2$. So, the numerical results in Table 2 confirm the theoretical results stated in Theorem 3.

Table 2: Numerical results for $\|\mathbf{RES}_n(t)\|_\infty$ with $\Delta = 10$

n	h	$d = 3$	Ratio	CPU time(s)	$d = 2$	Ratio	CPU time(s)
4	2.50000	$1.91e-4$	–	0.343	$1.01e-3$	–	0.341
8	1.25000	$2.09e-5$	3.19	0.562	$1.38e-4$	2.87	0.515
16	0.62500	$1.67e-6$	3.65	1.373	$1.86e-5$	2.89	1.357
32	0.31250	$1.20e-7$	3.80	5.538	$2.46e-6$	2.92	5.491
64	0.15625	$7.80e-9$	3.94	27.690	$2.90e-7$	3.08	27.082

As it is clear from the graphical and tabulated results, the proposed method can be successfully employed to solve the VIEs (1).

7 Conclusion

In this paper, the problem of the steady activation of a skeletal muscle has been investigated. Applying the numerical technique based on the integral operational matrix of the LBRIs, the approximate solution of the nonlinear VIE governing the problem was obtained. One of the advantages of the proposed method is that the FH interpolants are infinitely smooth rational interpolants and involve polynomial interpolants when $d = n, n-1$. Moreover, without using collocation points, the VIE (1) is reduced to a system of nonlinear algebraic equations. Numerical results confirmed the obtained theoretical results of Theorem 3. Thus, the method can be successfully employed to approximate the nonlinear VIEs with acceptable accuracy and computational times.

Acknowledgements

Authors are grateful to there anonymous referees and editor for their constructive comments.

References

[1] Abdi, A. and Hosseini, A. *The barycentric rational difference-quadrature scheme for systems of Volterra integro-differential equations*, SIAM J. Sci. Comput. 40 (2018), A1936–A1960.

[2] Berrut, J.P. *Rational function for guaranteed and experimentally well-conditioned global interpolation*, Comput. Math. Appl. 15 (1988), 1–16.

[3] Berrut, J. P., Hosseini, S. A. and Klein, G. *The linear barycentric rational quadrature method for volterra integral equations*, SIAM J. Sci. Comput. 36 (2014), A105–A123.

[4] Floater, M.S. and Hormann, K. *Barycentric rational interpolation with no poles and high rates of approximation*, Numer. Math. 107(2) (2007), 315–331.

[5] Gabriel, J.P., Studer, L.M., Rüegg, D.G. and Schnetzer, M.A. *A mathematical model for the steady activation of a skeletal muscle*, SIAM J. Appl. Math. 68 (2008), 869–889.

[6] Klein, G. and Berrut, J.P. *Linear barycentric rational quadrature*, BIT, 52 (2012), 407–424.

[7] Liu, H., Huang, J., Pan, Y. and Zhang, J. *Barycentric interpolation collocation methods for solving linear and nonlinear high-dimensional Fredholm integral equations*, J. Comput. Appl. Math. 327 (2018), 141–154.

[8] Maleknejad, K., Torabi, P. and Mollapourasl, R. *Fixed point method for solving nonlinear quadratic Volterra integral equations*, Comput. Math. Appl. 62 (2011), 2555–2566.

[9] Phillips, G.M. *Interpolation and approximation by polynomials*, CMS Books in Mathematics, Springer, New York, NY, 2003.

[10] Studer, L.M., Ruegg, D.G. and Gabrie, J.P. *A model for steady isometric muscle activation*, Biol. Cybern. 80 (1999), 339–355.

[11] Torkaman, S., Heydari, M., Loghmani, G. B. and Ganji, D.D. *Barycentric rational interpolation method for numerical investigation of magnetohydrodynamics nanofluid flow and heat transfer in nonparallel plates with thermal radiation*, Heat Transfer-Asian Research, 49 (2020), 565–590.

[12] Torkaman, S., Heydari, M., Loghmani, G.B. and Wazwaz, A.M. *Numerical investigation of three-dimensional nanofluid flow with heat and mass transfer on a nonlinearly stretching sheet using the barycentric functions*, Int. J. Numer. Methods Heat Fluid Flow. 31 (2020), 783–808.

[13] Torkaman, S., Loghmani, G.B., Heydari, M. and Rashidi, M.M. *Novel numerical solutions of nonlinear heat transfer problems using the linear barycentric rational interpolation*, Heat Transfer-Asian Research, 48 (2019), 1318–1344.

[14] Torkaman, S., Loghmani, G.B., Heydari, M. and Rashidi, M.M. *An effective operational matrix method based on barycentric cardinal functions to study nonlinear MHD nanofluid flow and heat transfer*, Int. J. Mech. Eng. 5 (2020,) 51–63.

How to cite this article

Torkaman, S., Heydari, M. and Loghmani, G.B., An operational matrix method for solving a class of nonlinear Volterra integral equations arising in steady activation of a skeletal muscle. *Iran. j. numer. anal. optim.*, 2023; 13(2): 336-353. https://doi.org/10.22067/ijnao.2022.73126.1069